

Reorientation in newly formed fission fragments

G.F. Bertsch

*Department of Physics and Institute of Nuclear Theory,
University of Washington, Seattle, Washington 98915, USA **

The strong quadrupolar component of the Coulomb field between newly formed fission fragments can affect the internal energy of the fragments and their angular momentum. Previous estimates of these effects gave contradictory conclusions about their magnitude. Here we calculate them by solving the time-dependent Hamiltonian equation for the daughter ^{100}Zr produced in the fission reaction $n + ^{235}\text{U} \rightarrow ^{136}\text{Te} + ^{100}\text{Zr}$. The Hamiltonian was constructed from the projected angular momentum eigenstates of an aligned deformed mean-field configuration. For typical initial conditions, the average angular momentum of the lighter fragment increases by 1.5 - 3 units.

Introduction. The strong Coulomb field in early post-scission fragment interactions could induce transitions that change the J -population before the neutron and gamma emission cascade starts. This question was addressed in early publications [1, 2] and follow-up studies (eg., [3, 4]) using similar methods to Ref. [1]. There the orientation of the two fragments at the scission point was treated by classical mechanics; the change in angular momentum was attributed to the torque from the Coulomb field of the partner fragment. In Ref. [2] the process was treated as in heavy-ion reaction theory where the nuclei are excited by their mutual Coulomb fields [5]. These two studies came to opposite conclusions: Ref. [1] found that the generated angular momentum was comparable to what was observed, but Ref. [2] found that the post-scission Coulomb field had little effect on the final states of the fragments. None of the studies to date have used the improved theoretical tools that we now possess based on self-consistent mean-field theory (SCMF) [6]. In this note we will examine the effect of the Coulomb field from the partner nucleus on a typical SCMF configuration of a scission product. These configurations are deformed with the deformation axis aligned along the fission direction. As a result they consist of a coherent superposition of angular momentum states, each having a vanishing angular momentum about the fission axis. We construct Hamiltonian matrix in that space of angular momentum eigenstates. The driving term that changes the composition of the wave function is the time-dependent Coulomb field from the other daughter nucleus.

Hamiltonian. The Hamiltonian basis is composed of angular momentum eigenstates defined by projection from the deformed initial configuration. The decomposition was carried out in Ref. [7] for the purpose of determining the importance of deformation in the final state and the effect of the alignment on the gamma decays in the final state. The probability P_J of angular momentum J was found to be very well approximated by the

spin-cutoff model¹

$$P_J \sim (2J + 1) \exp(-J(J + 1)/2\sigma^2). \quad (1)$$

We assume that the intrinsic deformed configuration is invariant under time reversal and contains only even angular momenta. The average angular momentum was estimated in Ref. [7] as

$$\langle J^2 \rangle \approx 0.3A^{3/2}\beta \quad (2)$$

where A is the number of nucleons in the fragment and β is the deformation parameter, which we define in terms of the mass quadrupole moment $Q_0 = \langle 2z^2 - (x^2 + y^2) \rangle$ as

$$\beta = \frac{\sqrt{5\pi}A^{5/3}}{3r_0^2}Q_0 \quad (3)$$

with $r_0 = 1.2$ fm.

The Hamiltonian consists of a rotational term H^{rot} together with term coupling to the quadrupole field of the partner nucleus H^Q ,

$$H = H^{\text{rot}} + H^Q. \quad (4)$$

The first term has the matrix elements

$$H_{JJ'}^{\text{rot}} = \left(\frac{\hbar^2}{2\mathcal{I}} \right) J(J + 1)\delta_{JJ'}. \quad (5)$$

where the moment of inertia \mathcal{I} may be estimated² as

$$\mathcal{I} = \frac{1}{2}\mathcal{I}_{\text{rig}} \quad (6)$$

with [9, Eq. 4-104]

$$\mathcal{I}_{\text{rig}} = \frac{2}{5}A^{5/3}Mr_0^2(1 + \beta/3). \quad (7)$$

¹ See also Ref. [8].

² There will be an additional small contribution from the orbital angular momentum of the two fragments about the center of mass.

The coupling to the quadrupole field at the daughter nucleus (and arising from the partner nucleus) is mediated by the electric quadrupole operator

$$\hat{Q}_e = e \sum_p (2z_p^2 - x_p^2 - y_p^2). \quad (8)$$

Its matrix elements are estimated in the rotor model as [9, Eq. (4-68a)]

$$\langle J' | \hat{Q}_e | J \rangle = \frac{1}{10} \sqrt{(2J+1)(2J'+1)} (J0J'0 | 20)^2 Q_e. \quad (9)$$

Here Q_e is the expectation value of the operator in the intrinsic state. The approximate relation to the mass quadrupole moment is

$$Q_e \approx \frac{eZ}{A} Q_0. \quad (10)$$

The Hamiltonian matrix elements of the quadrupole interaction are given by

$$H_{J,J'}^Q = V_Q \langle J' | \hat{Q}_e | J \rangle \quad (11)$$

where the Coulomb field strength V_Q depends on the separation R between the centers of mass of the two fragments as

$$V_Q(t) = \frac{Z_2 e}{2R^3}. \quad (12)$$

Here Z_2 is the charge of the partner nucleus.

The time evolution of $R(t)$ is treated classically by the Newtonian force equation,

$$\frac{d^2 R}{dt^2} = \frac{M_1 + M_2}{M_1 M_2} \frac{Z_1 Z_2 e^2}{R} \quad (13)$$

Finally, we solve the time-dependent Hamiltonian equation

$$i\hbar \frac{d\psi}{dt} = H\psi \quad (14)$$

where ψ is the vector of J -amplitudes and H has the explicit time dependence coming from V_Q .

Before carrying out the numerical solution of the equations of motion, we note some of the relevant energy scales in H . In the main example below, we will treat a case with a rather large deformation, $\beta = 0.5$. The initial energy in the quadrupole field is

$$E_Q \approx \frac{eZ_1 Z_2}{R^3(0)} Q_e \approx 3.5 \text{ MeV} \quad (15)$$

to be compared with the rotational energy of the initial configuration,

$$\sum_J P_J \left(\frac{\hbar^2}{2\mathcal{I}} \right) J(J+1) \approx 4 \text{ MeV}. \quad (16)$$

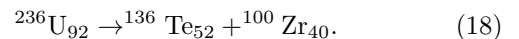
Since the two terms in H are comparable, the dynamical equations should be integrated numerically rather than relying on a perturbative treatment. However, we should not be surprised if the average angular momentum is slow to change. This follows from the structure of the Hamiltonian in the limit where V_Q is constant and H^{rot} can be ignored. Then the Hamiltonian matrix is tridiagonal with matrix elements approaching $H_{J,J} \approx V_Q Q_e / 4$ and $H_{J,J+2} \approx 3V_Q Q_e / 8$ as J becomes large. This is similar to the discretized Hamiltonian for a particle in a one-dimensional box. If the initial wave function is smooth and spread over many states, the subsequent evolution will be a diffusive expansion of the wave packet rather a displacement one way or the other.

In the absence of an external field, the quadrupole moment will undergo oscillations due to the changing relative phases of the J -states, but without any corresponding change in their probabilities. The period of the oscillation can be roughly estimated as

$$\tau = \frac{\pi \mathcal{I}}{\hbar \langle J \rangle} \approx 1200 \text{ fm/c}, \quad (17)$$

which longer than the interaction time scale for V_Q .

Application. To set the parameter values, we consider a typical fission decay



and examine the evolution of the $^{100}\text{Zr}_{40}$ daughter nucleus. The initial conditions for the separation coordinate are taken as $R = 17 \text{ fm}$ and $dR/dt = 0$ at $t = 0$. Fig. 1 shows the separation of the fragments as a function of time. One sees that V_Q will become small on a time

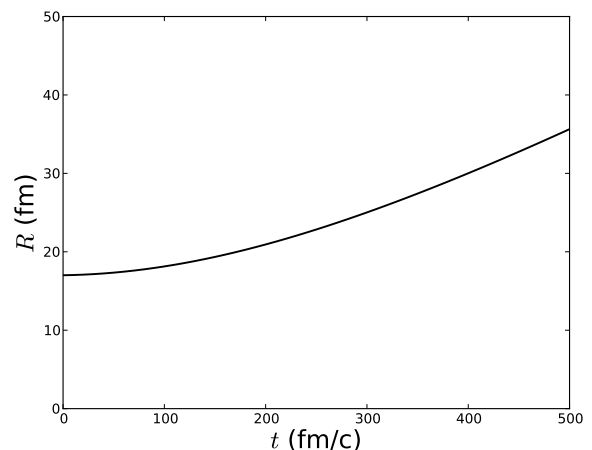


FIG. 1: Separation of the two fission fragments as a function of time.

scale of a few hundred fm/c due to its cubic dependence on R^{-1} .

The deformation of the lighter fragment might be very large. A recent study with time-dependent mean-field theory [10] found deformations in the range $\beta = 0.55 - 0.7$. In a pioneering early study of the statistical model of scission [14], it appeared that $\beta \approx 0.6$ was favored for the light fragment. For the present modeling, we will show details of the Hamiltonian evolution taking $\beta = 0.5$ in Eq. (2) and (3). From Eq. (2), the average angular momentum is given by $\langle J^2 \rangle^{1/2} \approx 12$. This is much larger than estimates based on characteristics of the neutron- and gamma-decay cascades of the daughter nuclei, so we will consider initial states with lower $\langle J \rangle$ as well. For the present example, the J -amplitudes are truncated beyond $J = 24$, resulting in a 13-dimensional Hamiltonian. The relative amplitudes in the initial wave function are taken as $a_J = P_J^{1/2}$ from probabilities determined by Eq. (1). For the other parameters in the Hamiltonian, the electric quadrupole moment is $Q_e = 4.7$ e-b and the moment of inertia is $\mathcal{I} = 17.5 \text{ MeV}^{-1} \hbar^{-2}$ from Eq. (5).

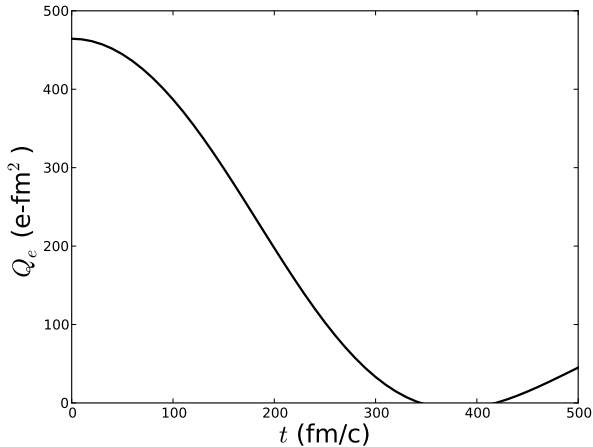


FIG. 2: Electric quadrupole moment of the lighter fragment as a function of time after scission.

We next carry out the numerical integration of Eq. (14) with the $V_Q(t)$ from Fig. (1). Fig. 2 shows the expectation value of the quadrupole moment as a function of time. Fig. 3 shows the corresponding average angular momentum. One sees that it increases significantly in the first few hundred fm/c reaching a steady value state by ~ 500 fm/c. Fig. 4 compares the final J distribution with the initial distribution. The position of the peak is shifted upward by about 5 units, and the average by 3 units.

Parameter variation There is abundant evidence from the gamma cascade in the excited daughter nuclei [11–13] that the average initial angular momentum is much smaller than what we found with our parameterization based on $\beta = 0.5$. It would therefore be informative to examine the dependence on the parameter values. Table

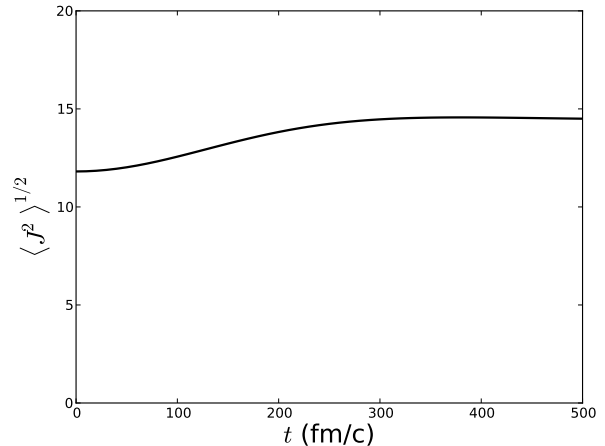


FIG. 3: Mean square angular momentum as a function of time after scission.

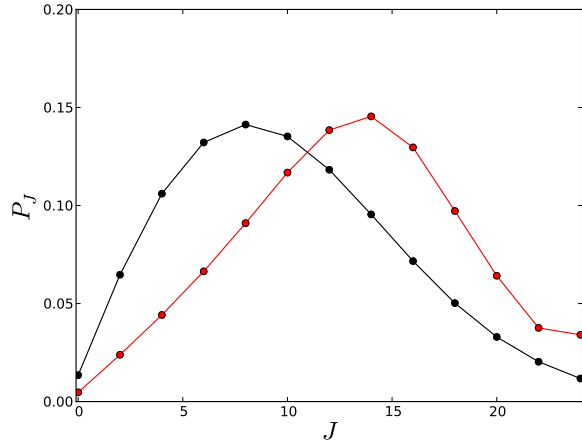


FIG. 4: Angular momentum decomposition of the wave function of the lighter fragment. The black and red circles are probabilities at $t = 0$ and 500 fm/c, respectively.

I shows the effect of varying some of model assumptions. The first entry A corresponds to the assumptions underlying the example from the previous section. The first parameter we varied is the moment of inertia, changing it by a factor of 2. There is no change increasing it, and a mild decrease when it is smaller. Thus, the results are rather insensitive to \mathcal{I} , provided it is not far from the physical value. The next change we considered is in the initial angular momentum distribution. Our distribution was determined assuming that the deformation axis of the daughter nucleus was perfectly aligned with the fission axis. In fact early theory based on classical concepts sometimes invoked excitation of a bending degree of freedom to account for the angular of the fragments. In our

	Q_e	\mathcal{I}/\hbar^2	$\langle J^2 \rangle^{1/2}$		ΔJ
			0	500	
A	470 e-b	17.5	11.8	14.5	2.7
B	470	35.0	11.8	14.5	2.7
C	470	8.8	11.8	13.5	1.7
D	470	17.5	6.0	8.7	2.7
E	235	16.1	6.0	7.4	1.4

TABLE I: Angular momentum at $t = 0$ and $t = 500$ fm/c under various sets of Hamiltonian parameters and initial wave function. A: the set with results shown in Figs. (6-8); B,C: same as A except for moment of inertia; D: same as A except for initial angular momentum distribution; E: Hamiltonian parameters given by Eq. (2,3,6) and (7) for $\beta = 0.25$.

formalism, inclusion of amplitudes of configurations such as depicted in Fig. 3 of Ref. [3] would delocalize the alignment of the axes and thereby lower the angular momentum content of the deformed wave packet. To explore this degree of freedom, we arbitrarily decreased the average angular momentum by a factor of two, changing σ in Eq. (1) by about that amount. The results are shown in entry D. Both angular momenta are much smaller, but the increase during the post-scission acceleration remains the same. The last variation we examined is to reduce β by a factor of two and change all the Hamiltonian parameters accordingly. The resulting reorientation effect is now reduced, adding only 1.4 units to the average.

Conclusion The main determinant of the angular momentum gain of fission fragments during the post-scission acceleration is their initial deformation and orientational alignment. The magnitude of the gain is of the order 1-3 units, which small not completely negligible compared to values 6-12 units at the scission point. We conclude

that the mechanism studied here would be significant if the theory of the angular momentum generation were reliable to the 10% level. However, in view of the much larger uncertainties in present theory, the reorientation effect can probably be ignored. The computer codes used to generate Figs. 2-4 are provided in the Supplementary Material [15].

Acknowledgment. The author thanks T. Kawano for discussions that led to this work.

* Electronic address: bertsch@uw.edu

- [1] M.M. Hoffman, Phys. Rev. **133**, B714 (1964).
- [2] J.B. Wihelmy, E. Cheifetz, R.C. Jared, et al., Phys. Rev. C **5** 2041 (1972).
- [3] J. Rasmussen, W. Nörenberg, and H. Mang, Nucl. Phys. **A136** 465 (1969).
- [4] S. Misticu, et al., Phys. Rev. C **60** 034613 (1999).
- [5] K. Alder, et al., Rev. Mod. Phys. **28** 432 (1956).
- [6] M. Bender and P-H. Heenen and P-G. Reinhard, Rev. Mod. Phys. **75** 121 (2003).
- [7] G.F. Bertsch, T. Kawano, and L.M. Robledo, arXiv:1810.13429.pdf (2018).
- [8] L. Bonneau, et al., Phys. Rev. C **75** 064313 (2007).
- [9] A. Bohr and B.R. Mottelson, *Nuclear Structure Vol. II*, (Benjamin, Reading, 1975).
- [10] A. Bulgac, S. Jin, K. Roche, et al., arXiv:1800:00694 (2018).
- [11] R. Capote, et al., Nucl. Data Sheets **100** 3107 (2009).
- [12] I. Stetcu, et al., Phys. Rev. **90** 024617 (2014).
- [13] J. Randrup and R. Vogt, Phys. Rev. C **989** 0443601 (2014).
- [14] B.D. Wilkins, et al., Phys. Rev. C **14** 1832 (1976).
- [15] The file of codes is available from the author prior to publication in a Supplementary Material folder.